POLITECNICO DI TORINO
Repository ISTITUZIONALE

Operationalizing resilience for sustainable infrastructure governance across the life cycle

Original
Operationalizing resilience for sustainable infrastructure governance across the life cycle / Domaneschi, M., Kopiika, N., Di Bari, R., Cavallaro, P., Villa, V., Argyroudis, S., Mitoulis, S.. - In: COMMUNICATIONS ENGINEERING. - ISSN 2731-3395. - (2026). [10.1038/s44172-026-00794-2]

Availability:
This version is available at: 11583/3017070 since: 2026-10-27T14:07:12Z

Publisher:
Springer Nature

Published
DOI:10.1038/s44172-026-00794-2

Terms of use:

This article is made available under terms and conditions as specified in the corresponding bibliographic description in the repository

Publisher copyright

(Article begins on next page)

03 November 2026

communications engineering

A Nature Portfolio journal

Article

Article in Press

https://doi.org/10.1038/s44172-026-00794-2

Decision-oriented resilience for sustainable infrastructure across the life cycle

Check for updates

Marco Domaneschi[1], Nadiia Kopiika[2,3], Roberta Di Bari[2,3], Paola Cavallaro[1], Valentina Villa[1], Sotirios Argyroudis[3,4] & Stergios-Aristoteles Mitoulis[2,3]

Sustainability and resilience expectations for infrastructure are escalating faster than the regulatory frameworks meant to deliver them. This mismatch is most acute for ageing critical infrastructure. Yet, adaptation decisions remain fragmented because resilience and sustainability operate on fundamentally different temporal domains: resilience captures short-term recovery dynamics and service continuity. Instead, sustainability evaluates long-term impacts across their life cycle. Here, we depart from this temporally disjoined approach. Instead of analysing trade-offs between resilience and sustainability metrics separately, we introduce a unified decision-oriented framework that integrates short-term recovery dynamics, representing resilience, with long-term life-cycle performance, expressing sustainability, within a common optimisation structure that links these temporal dimensions. We formulate resilience as a recovery-based variable linked to retrofit implementation and integrate it with Life Cycle Assessment (LCA), Life Cycle Cost (LCC), and multi-criteria decision analysis (MCDA) to support infrastructure decision-making across the life cycle. To the best of our knowledge, existing decision frameworks have not explicitly integrated resilience and sustainability across these temporal domains within a unified optimisation framework. Applied to a landmark ageing bridge, the framework evaluates six adaptation strategies under competing resilience, cost, carbon, and longevity objectives. Our results show that system level transformation with limited structural intervention can outperform conventional strategies, achieving stronger tradeoffs across resilience, environmental impact, cost, and service life extension. These findings provide actionable evidence for extending the lifespan of ageing infrastructure, while reducing environmental footprints. Thus, they offer a scalable pathway for aligning infrastructure adaptation with sustainability and resilience objectives under real-world constraints.

The progressive ageing of transport infrastructure poses urgent challenges for engineering, asset management, and policymaking, with populations becoming increasingly vulnerable to breakdowns in key systems due to the climate crisis and rapid urban growth[1]. In Europe, much of the bridge stock was constructed between the 1950s and the 1980s, and is now operating beyond its original design life, often under service conditions markedly different from those anticipated at the time of design and construction[1–3]. Accelerating drivers of deterioration include long-term material degradation, increasing traffic loads, and the increasing frequency and intensity of climate-related hazards[4–6].

Recent devastating failures have underscored the magnitude of these risks. For example, the collapse of the Francis Scott Key Bridge in Baltimore (2024) resulted in economic losses amounting to billions of USD due to port closures and insurance claims[7,8]. The tragic collapse of the deteriorated Polcevera Viaduct, also known as the Morandi Bridge, in Genoa led to 43 fatalities and severe disruption of the transport network[9,10].

[1]Department of Structural, Geotechnical and Building Engineering, Politecnico di Torino, Turin, Italy. [2]Centre for Global Infrastructure Resilience, The Bartlett School of Sustainable Construction, University College London, London, UK. [3]MetaInfrastructure, London, UK. [4]Brunel University of London, London, UK. e-mail: s.mitoulis@ucl.ac.uk

Recent literature has developed frameworks that link resilience and sustainability in infrastructure management. For example, the integrated sustainability and resilience assessment model by Roostaie et al. demonstrates the joint evaluation of hazard resistance and life cycle environmental performance[11]. Mitoulis et al. introduced sustained resilience as a unifying property that transcends conventional resilience and sustainability, capturing the capacity of the built environment and cities to accumulate, adapt and evolve through successive cycles of disruption and change while sustaining function throughout their life cycle[12,13]. Subsequent studies have further expanded this integration by considering both static and dynamic aspects of resilience[11] and developing resource-aware probabilistic frameworks for climate-resilient networks and decision-making[14]. On a global scale, Wiedenhofer et al.[15] quantified the material stocks, flows, and embodied greenhouse gas emissions associated with mobility infrastructure, underscoring the importance of life cycle carbon accounting in infrastructure renewal[16].

Specific integrated decision-making frameworks have also been developed, particularly within the sustainability domain, for example, for bridge retrofit and post-event repair selection[17], and within the structural resilience domain, where life cycle performance, reliability, cost, and recovery are incorporated into infrastructure decision processes[18,19]. These studies provide important methodological foundations, but differ from the present formulation in their decision context and treatment of resilience. Bocchini and Frangopol focused on post-disaster restoration and resource allocation in bridge networks following acute hazard events, while Dong and Frangopol developed performance-based resilience and sustainability formulations centered on hazard-induced damage, fragility, and life cycle structural performance. Tapia and Padgett[17] integrated sustainability considerations into bridge retrofit and post-event repair selection, but within a hazard-related damage and loss framework.

In contrast, the present study addresses retrofit planning under progressive deterioration, where resilience is formulated as an implementation-dependent recovery variable associated with intervention sequencing, service continuity, and operational recovery, and is jointly evaluated with life cycle environmental impact, cost, and expected service life. Within this broader context, prestressed and post-tensioned concrete bridges present particular vulnerabilities. Once celebrated for their efficiency and slender aesthetics, these structures are susceptible to creep, shrinkage, prestress losses, and tendon corrosion can progressively impair stiffness and load-carrying capacity[20]. Traditional inspection approaches, visual or intrusive, struggle to support continuous, network-scale management of these issues[21]. This has driven the adoption of non-invasive, resilience-oriented assessment methodologies, including data-intelligence driven methods for damage diagnosis and performance prediction[22], 3D laser scanning and CNNs for structural integrity evaluation of aging steel bridges[23], high-resolution remote sensing (drone photogrammetry, terrestrial laser scanning), probabilistic finite-element modeling and multi-criteria decision analysis for retrofit evaluation[5,24–26]. Advances in low-carbon and resilient construction materials offer new strengthening options[27], while evidence from building sectors shows that reuse, recycling and circularity indicators can substantially reduce environmental impacts when embedded in design and procurement and retrofit alternatives for adaptation[28–31].

Despite major advances in assessment tools, a fundamental gap persists: practical decision frameworks rarely integrate scenario-based recovery trajectories, ISO-compliant life cycle assessment (LCA) and life cycle cost (LCC), and expert-informed multi-criteria decision analysis within a single methodological concept. Existing integrated decision-making frameworks are generally formulated either within hazard-driven or performance-based contexts, where resilience is derived from probabilistic damage and recovery models, or within sustainability-oriented approaches focused on life cycle environmental and economic indicators. As a result, adaptation decisions remain poorly aligned with low-carbon objectives, including material efficiency, waste minimization, reduced embodied emissions, and resilience gains that limit service disruption. In most cases, resilience is still treated as an outcome of hazard response rather than as a recovery-based decision variable that could be threat-agnostic. Thus, it is explicitly linked to intervention implementation processes and operational recovery trajectories.

The need for integrated resilience and sustainability decision frameworks has also been recognized in the literature and in international policy agendas. Ayyub[32,33], for instance, emphasizes that understanding the relationship between resilience and sustainability is essential for effective and cost-efficient infrastructure decision making, while also highlighting the multidimensional nature of their quantification. More recently, Sánchez Silva et al.[34] highlighted that resilience and sustainability may involve conflicting objectives across different temporal and decision domains, and emphasized the importance of systems thinking, multicriteria life cycle evaluation, and integrated decision making for evolving infrastructure systems. Similar priorities are reflected in international governance frameworks, which increasingly advocate the joint consideration of resilience, sustainability, and economic performance in infrastructure planning and adaptation[35–37].

Resilience and sustainability operate across different temporal domains[38]. Resilience captures short-term recovery dynamics and service continuity, while sustainability evaluates long-term impacts across the life cycle. In practical retrofit decision making, however, these dimensions are inherently interconnected. Strategies that minimize recovery time may not minimize environmental impacts or maximize service life, while interventions that optimize long-term durability may require prolonged closures and increased short-term disruption. The proposed framework addresses this gap by enabling the joint evaluation of recovery performance, environmental impact, cost, and expected service life within the same decision process.

We introduce an integrated resilience and sustainability decision methodology and apply it to six retrofit and adaptation scenarios for the Polyfytos Bridge in Western Macedonia, Greece, a landmark balanced cantilever bridge experiencing tendon corrosion and severe serviceability degradation[20,25,26] cycle costs, and service impacts, enabling context-sensitive, low-carbon retrofit choices. This approach provides a scalable, evidence-based foundation for prioritizing retrofit and renewal strategies across ageing bridge networks in Europe and beyond. Hence, the main contribution is the unified, decision-oriented framework in which resilience is formulated as a recovery-based decision variable associated with retrofit implementation and explicitly linked to life cycle environmental and economic performance through LCA and LCC within a consistent decision structure.

Methods

Reframing recovery, sustainability, and costs into unified decisions

The methodology (Fig. 1) establishes a unified, decision-oriented framework integrating structural performance, recovery dynamics, life-cycle environmental impacts, economic costs, and expected service life for retrofit and adaptation planning. Its main contribution lies in formulating resilience as an implementation-dependent recovery variable and explicitly coupling recovery-oriented resilience modeling with life-cycle environmental and economic assessment within a consistent comparative structure. While the individual components build on established resilience, LCA, LCC, and MCDA approaches, their integration enables retrofit and adaptation scenarios to be evaluated jointly in terms of recovery trajectories during implementation, environmental and economic performance, and long-term durability, rather than solely through structural performance or hazard response.

For the case study examined here, a detailed structural assessment has been established in prior work[21,39], using SAR interferometry, high-resolution photogrammetry, terrestrial laser scanning, and forensic investigations, providing quantitative evidence of deformation, cracking, and material degradation. Expert judgement was further elicited through a structured questionnaire capturing feasible intervention options, operational continuity requirements, procedural timings, and logistical constraints, with inputs provided as numerical estimates, categorical responses,

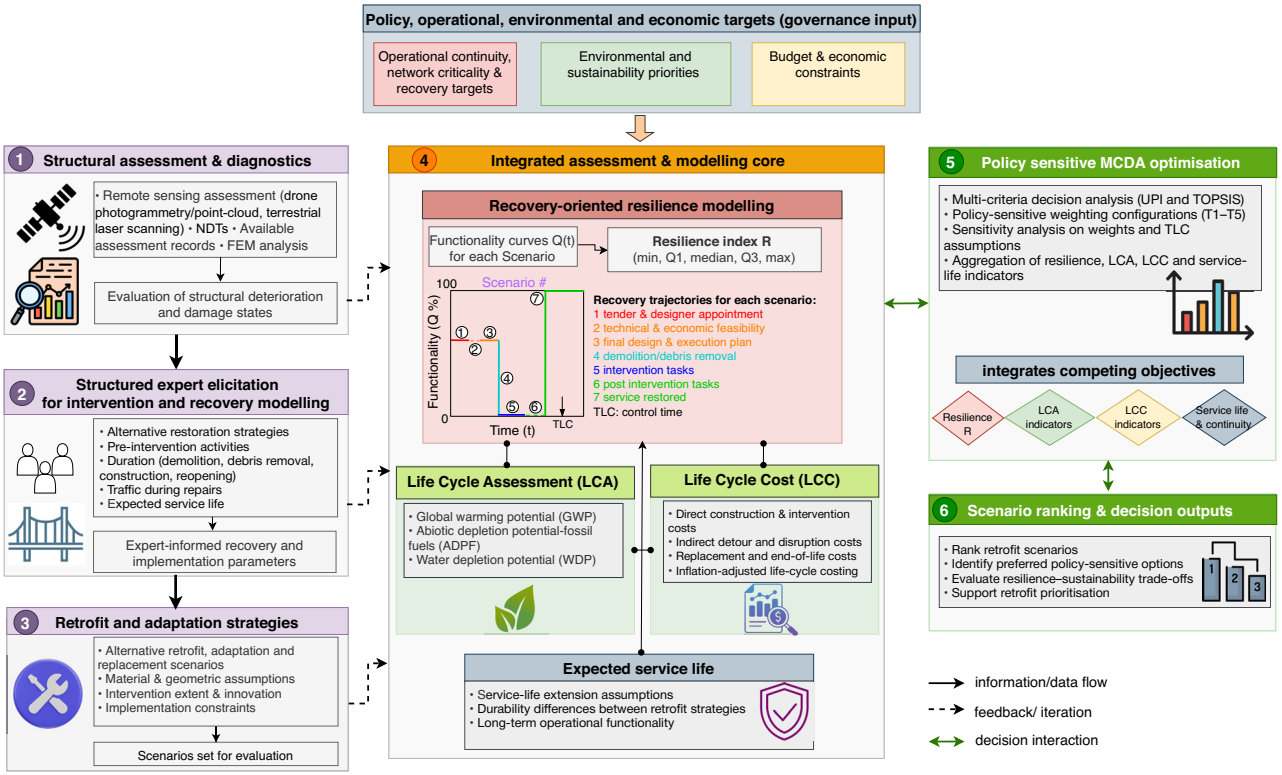


Fig. 1 | Decision-oriented framework for bridge adaptation under uncertainty. Presents an integrated six-step methodology linking structural diagnostics, expert-informed recovery modeling, sustainability assessment, and policy-sensitive decision optimization for ageing bridges. Governance inputs include operational continuity and recovery targets, environmental and sustainability priorities, and budget and economic constraints. Step 1 integrates structural assessment and diagnostics using remote sensing, non-destructive testing, inspection records, and numerical modeling to identify deterioration and damage states. Step 2 applies structured expert elicitation to define intervention and recovery parameters, including restoration strategies, implementation sequencing, intervention durations, operational continuity during works, and expected service life. Step 3 defines retrofit and adaptation scenarios, spanning repair, strengthening, and replacement strategies, while accounting for material assumptions, intervention extent, and implementation constraints. Step 4 represents the integrated assessment and modeling core. Recovery-oriented resilience modeling, i.e., hazard-agnostic, evaluates functionality-time recovery curves and derives resilience indices from expert-informed descriptors (minimum, quartiles, median, and maximum) relative to a control time representing acceptable recovery targets. Environmental and economic performance are quantified through LCA and LCC, including environmental indicators, such as global warming potential (GWP), abiotic depletion potential-fossil fuels (ADPF), water depletion potential (WDP), and direct, indirect, replacement, and end-of-life costs. Expected service life is evaluated through durability and long-term operational functionality assumptions. Step 5 integrates all criteria through policy-sensitive multi-criteria decision analysis (MCDA), while Step 6 ranks retrofit scenarios and supports retrofit prioritization[59–61].

free-text commentary, sketches, and supporting files. This combined evidence base supports the definition of retrofit and adaptation strategies spanning repair and replacement solutions with varying levels of intervention extent and system transformation. Resilience performance is quantified by modeling functionality-time recovery trajectories for each scenario, capturing recovery duration and service continuity under uncertainty. Environmental and economic performance is evaluated through LCA and LCC analysis, enabling consistent comparison of embodied impacts, resource use, and long-term costs. All indicators are subsequently weighted and aggregated using multi-criteria decision analysis, with explicit weighting and sensitivity analysis used to explore trade-offs between resilience, sustainability, cost, and service life and to identify preferred retrofit strategies under differing decision priorities. The following subsections formalize the theoretical and methodological components underpinning this unified approach.

Infrastructure assessment, retrofit, and adaptation strategies

The assessment combines accurate appraisal of the physical condition with the bridge's functional role in the transport network, projected service life, feasibility of available technologies and cost-benefit considerations[40]. Environmental objectives (e.g., minimizing material waste and embodied carbon and avoiding environmental harm) are incorporated as explicit decision criteria[17]. Within the scope of the case study bridge described in the Supplementary Note 1, six retrofit strategies were considered. They represent a broad spectrum of intervention approaches for ageing bridge decks, ranging from localized strengthening measures to partial and full deck replacement. The scenarios differ in terms of structural intervention extent, constructability, expected recovery profiles, environmental impact, and service life, and reflect realistic alternatives available to infrastructure owners. Figure 2 provides a schematic overview of the retrofit strategies analyzed.

The six retrofit strategies are summarized as follows. A detailed comparison of intervention type, Gerber joint treatment, external prestressing, traffic disruption, and degree of system transformation is provided in Supplementary Table 1.

- Scenario #1 is a hybrid repair strategy that preserves the cantilever beams, replaces the Gerber-type members with steel beams, and introduces external prestressing.
- Scenario #2 is a structural transformation strategy based on stay cable augmentation and partial replacement, aimed at redistributing forces and increasing redundancy.
- Scenario #3 is a preservation oriented external prestressing solution that retains the existing cantilevers and Gerber beams while rehabilitating slabs and half joints.

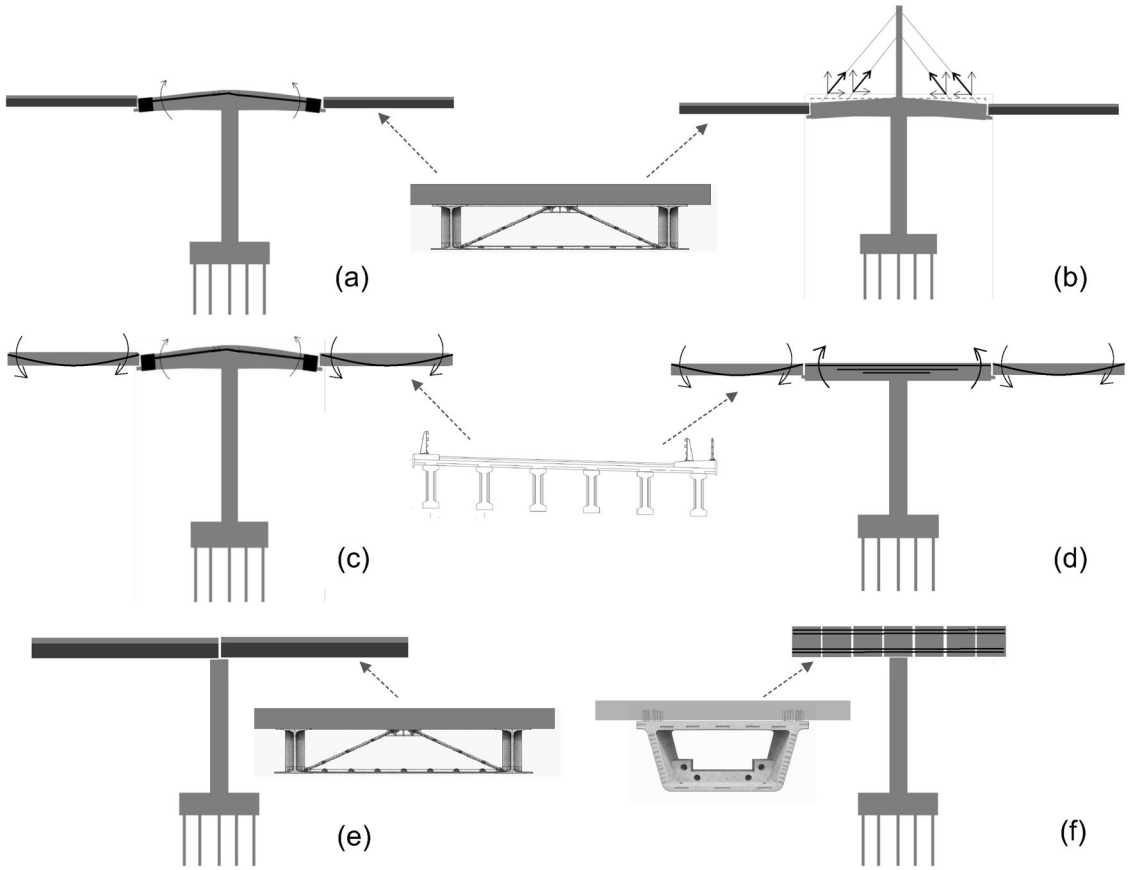


Fig. 2 | Retrofit scenarios for the defected part of the bridge deck. It is proposed that the balanced cantilever part of the deck can be retrofitted by: **a** Scenario #1 – hybrid intervention with preservation of cantilever beams, replacement of simply supported members with steel beams, and application of external prestressing. **b** Scenario #2 – stay cable augmentation with new pylons and stays anchored to the main piers to redistribute forces and increase structural redundancy. **c** Scenario #3 – external prestressing solution retaining cantilevers and simply supported beams with rehabilitation of slabs and half joints. **d** Scenario #4 – full replacement with a conventional prestressed concrete deck replicating the original static scheme with improved durability. **e** Scenario #5 – full replacement with a steel-concrete composite deck to reduce self-weight and accelerate construction. **f** Scenario #6 – full replacement with a prefabricated modular deck using dry joints for rapid installation and future reparability.

- Scenario #4 is a full replacement strategy with a conventional prestressed concrete deck, replicating the original static scheme with improved durability.
- Scenario #5 is a full replacement strategy with a steel concrete composite deck, aimed at reducing self-weight and facilitating construction.
- Scenario #6 is a prefabricated modular deck replacement using dry joints, aimed at rapid installation and future reparability.

While the paper focuses on the comparative assessment of these scenarios in terms of resilience, sustainability, and cost, detailed descriptions of the structural configuration, damage states addressed, and implementation constraints for the case study bridge are provided in Supplementary Note 1.

The evaluation of the alternative retrofit strategies was based on a global questionnaire administered between 2024 and 2025 gathered expert judgement from seven senior bridge specialists (practitioners and academics across six countries) on restoration strategies. For landmark infrastructure systems undergoing highly specialized retrofit interventions, empirical recovery datasets are rarely available, making expert elicitation essential for constructing realistic functionality-time recovery trajectories under uncertainty.

More than 50 experts were invited internationally, and seven completed responses were retained for analysis based on seniority (more than 10 years of relevant experience in bridge strengthening) and completeness. The elicited values should therefore be interpreted as expert judgement supporting comparative methodological evaluation and decision-making under uncertainties, rather than as statistically representative population-level estimates, consistently with structured expert elicitation approaches reported in the literature[41–43].

The structured expert elicitation combined quantitative estimates and qualitative inputs covering alternative intervention options, preparatory planning durations, demolition scope, operational continuity during works, task execution times, post-intervention administrative delays, and expected service life. Participants received a dedicated briefing package prior to completion; participation was voluntary and anonymized. The number of responses was deemed adequate given the depth of the questionnaire, which prioritized context-specific input from highly experienced experts rather than large response volumes, consistent with best practice in expert elicitation studies[44]. The elicited information was used to parameterize recovery profiles, uncertainty ranges, and operational constraints adopted in the resilience, life cycle, and decision analyses presented in the Results section. Full details of the questionnaire are provided in Supplementary Note 2.

Hence, the elicitation exercise was designed as a structured expert consultation process rather than a conventional survey aimed at statistical inference. The objective was to obtain high-quality, context-specific estimates of recovery trajectories, implementation durations, and operational constraints for a landmark ageing bridge system for which empirical recovery datasets are limited. The exercise required substantial technical engagement and interdisciplinary expertise in bridge assessment, retrofit engineering, resilience analysis, and life-cycle evaluation. Consequently, expert relevance and depth of input were prioritized over sample size.

Expert elicitation informed the definition of retrofit options, recovery durations, operational continuity assumptions, implementation sequencing, and expected service life. It did not define material quantities, environmental characterization factors, or unit cost data, which were derived from engineering inventories, environmental datasets, and cost sources. Accordingly, expert judgement affects the resilience trajectories and service-life criterion, while LCA and LCC values are calculated from the inventory and cost model described below.

Fit-for-purpose resilience assessment

Resilience is interpreted within a decision-oriented adaptation framework associated with progressive deterioration and planned retrofit implementation, rather than within a hazard-driven fragility-based framework. Thus, the objective is to evaluate recovery and service continuity under alternative intervention strategies, rather than probabilistic damage evolution resulting from external hazards.

According to a general approach, resilience is herein modeled as a performance metric to express the ability of infrastructure to recover their functionality following disturbances within a specified control period. As per Bruneau et al.[45], resilience R is as:

$$R = \frac{1}{T_{LC}} \int_{T_0}^{T_0+T_{LC}} Q(t)dt \quad (1)$$

where $Q(t)$ is the normalized functionality (0–1); T_0 marks the start of the retrofit process, including administrative phases, such as design, permitting, and procurement; T_{LC} is the control time, i.e., the duration over which the recovery trajectory is evaluated, measured from T_0; T_{LC} represents the maximum acceptable time for the complete restoration of the bridge's functionality level and is selected based on strategic, operational, and societal requirements[46]. In setting T_{LC}, the strategic role of the bridge within the transport network and the degree of network redundancy are considered by the owner/operator. Based on these considerations, restoration objectives, recovery targets, and implementation guidance are established[47–51], typically aligned with empirical benchmarks from similar restoration projects and practical feasibility constraints, such as procurement lead times and constructability limits. The recovery time T_{RE} is treated as an uncertain expert elicited variable, reflecting variation in intervention duration, administrative delays, and operational continuity assumptions. Variation is represented through descriptive recovery conditions derived from the elicitation, namely, minimum, first quartile, median, third quartile, and maximum values. While resilience targets aim to achieve $T_{RE} \le T_{LC}$, in practice, T_{RE} may exceed T_{LC} under adverse conditions. In such cases, the functionality-time curve is truncated at T_{LC}, such that $Q(T_{LC}) < 1$. This ensures that the resilience integral remains well-defined over the fixed control horizon T_0, T_{LC} and reflects incomplete recovery within the acceptable time window. Scenarios with $T_{RE} > T_{LC}$ are therefore considered non-compliant with resilience targets[47–51].

The proposed framework considers functionality-time trajectories, derived from intervention sequencing, operational continuity assumptions, implementation constraints, and expert-informed recovery estimates, reflecting realistic retrofit conditions for the analyzed bridge system. For the resilience assessment, uncertainty originates from the expert elicited estimates of intervention duration, administrative delays, and operational continuity assumptions used to construct the functionality time trajectories. In practice, the selection of a reference control time requires balancing strategic importance, network redundancy, societal impacts of service disruption[50], and realistic implementation constraints. Prolonged closures of critical infrastructure assets can result in substantial detours, economic losses, and social disruption. Empirical evidence indicates that complex interventions on major bridges typically span on the order of 2–3 years, even when expedited. Representative cases include the Ponte San Giorgio (Genoa, Italy), where demolition, design and reconstruction were completed in 24–30 months; the West Seattle Bridge (USA), rehabilitated between March 2020 and September 2022 (~30 months); and the Arlington Memorial Bridge (Washington, DC, USA), whose major rehabilitation required approximately 30 months. To complement the resilience metric, a compliance ratio defined as $P(T_{RE} \le T_{LC})$ is introduced to quantify the possibility that a given intervention satisfies the recovery-time constraint under uncertainty. To assess the robustness of ranking outcomes under alternative recovery-policy assumptions, supplementary sensitivity analyses considering control times of 24 and 36 months were additionally performed.

Integration of sustainability

LCA and LCC analyses are used to quantify the environmental and economic performance of infrastructure restoration strategies over their entire life cycle. Since the assessment is conducted at the asset level and all proposed options are designed to restore the bridge to full operational capacity, the selected functional unit is one kilometer of bridge length. The selected unit allows for comparability of scenarios and scalability of costs and impacts for other case studies. Intervention scenarios may not be functionally equivalent in terms of durability and service life. However, they are designed with at least 50 years' service life. Performance differences are accounted in this study through explicit multi-criteria integration, rather than by assuming functional equivalence. The system boundaries of the analysis encompass the demolition and waste processing of damaged bridge components (in this study called C1-C4_old), raw material extraction and manufacturing, transportation, construction and installation processes (A1-13), elements replacement (B4) and end-of-life stages of newly installed elements (C1-C4_new), following standards specific for construction works (EN 15804 and EN 15643[52,53]). The environmental impacts caused by maintenance (Module B2) are disregarded, as they are deemed to be negligible and similar across the designed interventions. Consequently, they do not influence the ultimate decision-making process.

Impacts are assessed considering 50 years' observation time. The sum of these contributions provides the total life cycle environmental impact associated with each intervention strategy. Environmental impact categories considered typically include global warming potential, water use, fossil resource use, and mineral and metal resource depletion, as defined in EN 15804+A2[52]. Data sources may include environmental product declarations, generic life cycle inventory databases, and context-appropriate cost datasets, selected to ensure consistency and transparency of the assessment. Because of a lack of context-consistent data, it was not possible to perform a formal uncertainty analysis. Therefore, LCA and LCC are here performed with a deterministic approach. For LCC, temporal variabilities are considered. Specifically, costs have been adjusted to ensure temporal consistency over the observation time of the analysis using an appropriate inflation rate (2.8%). Moreover, to bring future nominal cash flows back to present value (PV), we have formally introduced a real discount rate of 4.0%. This specific rate represents the standard macroeconomic benchmark recommended by the European Commission's Cost-Benefit Analysis (CBA) guidelines for public infrastructure, civil engineering, and environmental projects. As a result, the equation providing the present value for LCC is the following:

$$PV(y) = C_{nom} \frac{(1+e)^y}{(1+r)^y} \quad (2)$$

where C_{nom} is the nominal cost (according to price statistics from the Greek construction costs' catalogue), e is the inflation rate and r is the real discount rate.

LCC analyses incorporate both direct and indirect economic components. LCC accounts for initial investment, maintenance, operational expenditures over 50 years' observation time, end-of-life costs. Differently from LCA, the scope of the LCC analysis has been extended. In addition to the direct costs associated with the interventions and their life cycle, cost analyses encompass indirect user costs that are precipitated by factors such as traffic disruptions and detours. Similarly to LCA, costs associated with maintenance are excluded on the basis that the activities in question are executed in a consistent manner across all the scenarios that have been

designed. A bill of materials is compiled for each intervention scenario to parameterize material production and end-of-life stages. Information on raw material extraction, manufacturing, and end-of-life options is obtained from manufacturers or established databases. Where multiple end-of-life scenarios are available, conservative assumptions are adopted to avoid underestimation of environmental impacts. Environmental impacts associated with material production and end-of-life stages are calculated as:

$$EI_{\substack{A1-A3\\C3-C4}} = \sum_{mat} Q_{mat}\, EI_mat_{\substack{A1-A3\\C3-C4}} \quad (3)$$

where $EI_{\substack{A1-A3\\C3-C4}}$ is the impact or cost of $A1$–$A3$ or $C3$–$C4$ stages; Q_{mat} is the quantity estimated of a specific construction material (mat). The quantity is expressed in the declared unit (du) of the environmental dataset. $EI_{mat,\substack{A1-A3\\C3-C4}}$ is the embodied impact/cost of the construction material, expressed in kg emission eq. or cost per declared unit.

Each intervention is associated with a specific on-site fabrication ($A5$ module). Information was collected for each fabrication regarding the machinery used, its power and how long it was used. This enables the estimation of the electrical energy consumed by each machine to be calculated:

$$I_{A5} = \sum_{mac} Q_{mac}\, I_{elec} \quad (4)$$

$$Q_{mac} = P_{mac}\, T_{mac}\, cf \quad (5)$$

where I_{A5} is the impact of $A5$ stage; Q_{mac} is the energy consumed by a specific machine (mac) in kWh; $I_{elec,A5}$ is the impact of the electricity (energy mix, country average), in kg emissions eq. or cost per kWh; P_{mac} is the machine power; T_{mac} is the usage time of the machine; cf is a correction factor (0.8) to consider that the machine does not work at its full power for the whole usage time. This formula is used only for LCA analysis. In fact, for LCC, the used cost data merges material and construction expenditures into one value.

Impacts due to elements replacement (B4) are calculated as by adding the impact of end-of-life of replaced material and elements I_{C3-C4} and impact of replacing elements I_{A1-A3}. In this study, it is assumed that the replaced and replacing materials and elements do not change over the 50 years' period. For instance, when the asphalt layer must be replaced, this will occur by demolishing the old asphalt layer and replacing this with the same type of asphalt.

Costs of B4 are adjusted considering an inflation rate of 2.8% and a real discount rate of 4.0%.

Impacts due to demolition ($C1$) I_{C1} are calculated similarly to $A5$, by considering energy consumption and the impact of the energy mix:

$$I_{C1} = \sum_{mac} Q_{mac}\, I_{elec} \quad (6)$$

Impact I_{C2} for $C2$, waste transport, is calculated considering the distance (D_{tr} in km) and impact per km I_{tr}. This value is multiplied by the number of trucks required. This is equivalent to the demolition material quantity Q_{dem} (expressed in t) divided by the nominal payload (mass) capacity of a standard heavy-goods vehicle, assumed as 44 t.

$$I_{C2} = \left(\frac{Q_{dem}}{44}\right) \sum_{tr} D_{tr}\, I_{tr} \quad (7)$$

End-of-life costs are also adjusted in order to evaluate future value with an inflation rate of 2.8% and a real discount rate of 4.0%.

After calculating each life cycle contribution, the total direct impacts are assessed and divided by 1.37 km (bridge length, chosen as functional unit for LCA and LCC analyses):

$$I_{LC,dir} = \frac{I_{A1-A3} + I_{A5} + I_{B4} + I_{C1} + I_{C2} + I_{C3-C4}}{1.37} \quad (8)$$

Indirect costs due to the traffic detour are calculated as the product of the total distance of each mean of transportation ($D_{\text{detour,tr}}$), expressed in kilometer and the cost of a kilometer traveled I_{tr} of each mean of transportation. All contributions of each mean of transportation tr are finally summed to derive the total indirect costs I_{ind}

$$I_{ind} = \sum_{tr} D_{detour,tr}\, I_{tr} \quad (9)$$

The resulting LCA and LCC indicators provide comparable metrics that can be integrated with resilience and structural performance measures within the MCDA. For the case study, indirect user costs were estimated using approximate traffic-demand and detour assumptions representative of local operating conditions. Average daily traffic was approximated as 10,000 vehicles per day based on local population and traffic characteristics of the nearby urban centers (Servia and Kozani), assuming traffic demand corresponding to approximately 15% of the combined population. The detour associated with the bridge closure was estimated as an additional travel distance of approximately 25 km based on route mapping using open sources. These estimates are intended to provide comparative planning-level indicators of disruption costs rather than detailed traffic-engineering forecasts. Since identical traffic-demand and detour assumptions were adopted across all retrofit scenarios, these parameters do not affect the relative ranking trends within the MCDA framework.

Multi-criteria decision analysis and optimization

MCDA is adopted to support the systematic comparison and ranking of alternative intervention strategies characterized by multiple, potentially conflicting objectives. Each adaptation solution $i \in S$, among the analyzed set S, is characterized by the following key dimensions:

(A) Resilience $R_i \in [0, 1]$, derived from the functionality-time curves and the structured expert elicitation. Resilience combines central tendency and upper-tail performance to capture both typical outcomes and robustness to implementation delays. Specifically, the median ($Q2$) of the functionality-recovery variability is used as the primary resilience indicator, representing the most likely restoration trajectory and is robust to outliers. The upper quartile ($Q3$) is incorporated as a secondary indicator to reflect near-worst-case delays and the propensity of a strategy to exceed the reference control time; options with large $Q3$ values are therefore penalized relative to alternatives with narrower dispersion. The median-based and upper-tail-based indicators are normalized and combined into a single resilience score using explicit weights (with greater emphasis typically assigned to the median), thereby balancing expected performance, robustness to adverse delays, and protection against unacceptable worst-case outcomes.

The mean and standard deviation of elicited responses are reported only as descriptive indicators of variation across expert judgements. They are not used to fit a probability distribution or to perform probabilistic propagation through the MCDA. For the baseline decision model, the median recovery trajectory represents central recovery behavior, while the upper quartile represents adverse recovery conditions.

(B) Life cycle cost LCC_i [EUR/km of bridge, aggregated index]. LCC incorporates both direct intervention expenditures and indirect user costs (e.g., detour-related travel time and vehicle operating costs). These two components are combined into a single LCC score. Component weights may be specified to reflect empirical estimates or stakeholder preferences.

(C) Life cycle assessment impact LCA_i [impact units, aggregated index]. Environmental performance is represented by an aggregated LCA index

constructed as a weighted sum of relevant impact categories selected to capture climate, resource depletion and water footprint. The present study includes, at a minimum, the following: global warming potential (GWP, kg CO_2-eq/km), abiotic depletion potential-minerals & metals (ADP minerals, or ADPM kg Sb-eq/km), abiotic depletion potential-fossil fuels (ADP fossil, or ADPF MJ/km), and water depletion potential (WDP, m^3 freshwater/km). Each category is weighted and assigned a policy-driven weight coefficient (w_i), explicitly reported and justified, and the aggregated LCA_i is then computed as a sum of all the categories, enabling tradeoff analysis and sensitivity testing of weighting choices. The weighting factors of this study are based on the environmental damage and planetary boundaries, the importance of impact categories in current policies and the underlying impact categories' uncertainties. Weighting factors do not strictly depend on the scope of the assessment[54].

(D) Expected service life L_i [years]. The remaining service life for each intervention is elicited from domain experts using structured protocols and represented as a central estimate with an associated uncertainty range. Service life estimates may be obtained from expert elicitation, historical performance, or engineering judgement, depending on data availability.

Next, *min–max normalization* is applied to rescale all variables onto a common [0, 1] range, ensuring consistent comparison across criteria with different units and magnitudes and enabling the construction of a composite index, as per Eq. 10:

$$\hat{X}_i = \frac{X_i - \min X}{\max X - \min X} \tag{10}$$

where $\hat{X}_i$ is normalized value of criteria X ($\hat{C}_i$, for cost criteria, $\hat{E}_i$ for environmental criteria, $\hat{R}_i$ for resilience criteria, $\hat{L}_i$ for extended service life criteria). This transformation preserves monotonicity, facilitates direct comparability across heterogeneous units, and yields intuitively interpretable bounds (best = 0 or 1, worst = 1 or 0 depending on direction). Since min–max normalization is performed relative to the analyzed set of retrofit alternatives, the resulting normalized values and rankings are scenario-set dependent. The rankings should therefore be interpreted as relative comparisons within the predefined decision space considered in this study.

Hence, the multi-objective optimization can be expressed as:

$$\max_{i \in S} \left(1 - \hat{C}_i, 1 - \hat{E}_i, \hat{R}_i, \hat{L}_i\right) \tag{11}$$

Min–max normalization was adopted to ensure transparent and consistent relative comparison among retrofit alternatives within the MCDA framework. Alternative normalization schemes, including z-score and target-based normalization, were considered; however, they were not deemed appropriate for the present application. Z-score normalization relies on statistically robust estimates of mean and standard deviation, which are not reliable for the limited number of analyzed alternatives, while target-based normalization would require the introduction of external benchmark values that are not consistently available across the considered resilience, environmental, economic, and service-life criteria. Furthermore, no extreme outlier behavior was observed among the analyzed alternatives that would lead to severe compression effects within the normalized criteria space.

Scalarization and unified performance index (UPI)

Since the Pareto set typically contains multiple non-dominated alternatives, an additional decision step is required to identify a single preferred solution. Scalarization methods convert the multi-objective problem into a single-objective one by aggregating the normalized criteria into a UPI. As a primary approach, a weighted-sum method is adopted:

$$J_i = w_C(1 - \hat{C}_i) + w_E(1 - \hat{E}_i) + w_R\hat{R}_i + w_L\hat{L}_i \tag{12}$$

where w_C, w_E, w_R, $w_L w_L \geq 0$ and $w_C + w_E + w_R + w_L = 1$. By varying the weight vector, the decision approach can reflect alternative policy priorities, for example, prioritizing resilience (larger w_R) or longevity (larger w_L) or emphasizing economic or environmental objectives (larger w_C or w_E, respectively). The specific weight vectors used in the sensitivity analysis ($T1$–$T5$) are defined explicitly as follows: $T1$ (equal weighting): $w_C = 0.25$, $w_E = 0.25$, $w_R = 0.25$, $w_L = 0.25$; $T2$ (economic priority): $w_C = 0.55$, $w_E = 0.15$, $w_R = 0.15$, $w_L = 0.15$; $T3$ (environmental priority): $w_C = 0.15$, $w_E = 0.55$, $w_R = 0.15$, $w_L = 0.15$; $T4$ (resilience priority): $w_C = 0.15$, $w_E = 0.15$, $w_R = 0.55$, $w_L = 0.15$; $T5$ (service-life priority): $w_C = 0.15$, $w_E = 0.15$, $w_R = 0.15$, $w_L = 0.55$. In this specification (Eq. 12), $\hat{C}_i$ and $\hat{E}_i$ denote min–max normalized cost and environmental impact (scaled so lower is better), while $\hat{R}_i$ and $\hat{L}_i$ denote normalized resilience and expected service life (scaled so higher is better); the terms are arranged so that larger J_i indicates superior overall performance. Within the decision framework, T_{LC} is treated as a soft constraint. Scenarios that exceed the control time are not excluded a priori but are penalized through reduced resilience scores and increased dispersion in recovery trajectories, allowing trade-offs between short-term recovery performance and long-term benefits (e.g., service life extension or reduced environmental impact) to be explicitly evaluated. Thus, $T_{RE} > T_{LC}$ denotes non-compliance with the recovery target, but not automatic exclusion from the decision space; instead, such cases are retained and penalized through reduced resilience scores and compliance characteristics.

It should be noted that the UPI is not intended to imply physical commensurability among resilience, life-cycle cost, environmental impact, and expected service life. These dimensions represent different value domains and cannot be reduced to a common physical unit. The scalarization in Eq. 12 should therefore be interpreted as a preference-based decision model that makes weighting assumptions explicit, rather than as a mechanistic equivalence among criteria. Consequently, the resulting rankings are conditional upon the adopted weighting scheme and decision context. The use of alternative weighting scenarios and complementary TOPSIS analysis was intended to assess the robustness of ranking outcomes under different stakeholder preferences. By making value judgements explicit through weights, control times, and uncertainty thresholds, the method enables transparent alignment between engineering choices and policy objectives within real-world regulatory and budgetary constraints.

TOPSIS robustness assessment and verification

To verify the robustness of the UPI ranking, the Technique for Order Preference by Similarity to an Ideal Solution (TOPSIS) was adopted as a complementary MCDA method. TOPSIS is widely used for ranking alternatives in decision problems involving multiple, conflicting criteria, and provides an interpretable closeness coefficient based on the relative distance of each alternative from ideal and anti-ideal solutions[55,56]. This is suitable for the present retrofit selection problem, where alternatives and tradeoffs are compared across resilience, LCC, environmental impact, and expected life-cycle. Compared with outranking methods, such as ELECTRE, TOPSIS avoids the need to define additional preference, indifference, and veto thresholds. Compared with compromise ranking methods, such as VIKOR, TOPSIS focuses on proximity to an ideal solution rather than on regret-based compromise assumptions. It is therefore used here as a robustness check of the weighted sum UPI ranking, rather than as a universally superior MCDA method.

TOPSIS evaluates each candidate by its geometric proximity to an ideal reference, which is the best possible performance on all normalized criteria, and its distance from an anti-ideal reference, which is the worst possible performance. For each solution i, the weighted Euclidean distances to the ideal A^+ and anti-ideal A^- are computed as follows:

$$D_i^+ = \sqrt{\sum_k w_k(\hat{x}_{ik} - A_k^+)^2} \tag{13}$$

$$D_i^- = \sqrt{\sum_k w_k(\hat{x}_{ik} - A_k^-)^2} \tag{14}$$

where $\hat{x}_{ik}$ denotes the normalized value of criterion k for solution i, w_k are the criterion weights, and A^+ and A^- denote the ideal and anti-ideal vectors

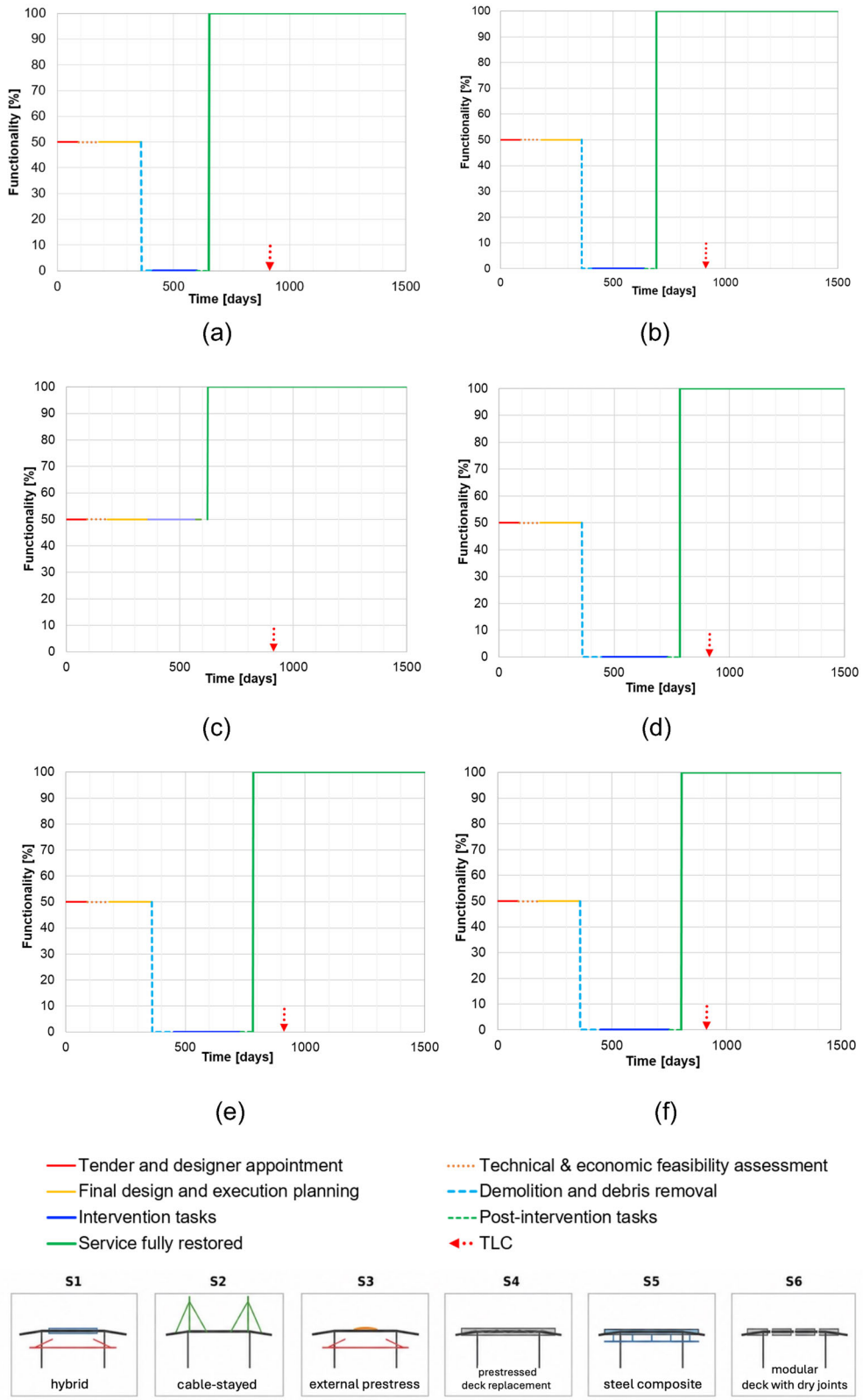


Fig. 3 | Functionality curves for six retrofit scenarios (median values, *Q*2). **a** Scenario #1; **b** Scenario #2; **c** Scenario #3; **d** Scenario #4; **e** Scenario #5; **f** Scenario #6. These ex-ante curves, constructed for comparative evaluation within a decision-oriented framework, illustrate distinct recovery profiles. Scenario #3 achieves full recovery in approximately 21 months while uniquely maintaining partial service throughout the intervention. Scenarios #1 and #2 recover efficiently in just under 23 months, whereas #4 and #5 take approximately 26 months, and #6 is the slowest at circa 27 months. All adaptation strategies are completed within the 30-month control time under median conditions, although several exceed this threshold under upper-quartile and maximum uncertainty conditions (see the variability details in Supplementary Note 3).

(defined according to the optimization direction of each criterion). The closeness coefficient is then computed using TOPSIS as:

$$CC_i = \frac{D_i^-}{D_i^+ + D_i^-} \quad (15)$$

where D_i^+ represents the weighted Euclidean distance of solution i from the ideal point $A^+ = (0,0,1)$, and D_i^- the weighted Euclidean distance from the anti-ideal point $A^- = (1,1,0)$. The closeness coefficient provides an interpretable measure of relative performance and is used to verify the weighted-sum ranking results in the case study.

Results and discussion

This section applies the proposed methodology to the Polyfytos bridge, using the deteriorated zone as a representative case for evaluating alternative retrofit strategies; detailed case-study information is provided in Supplementary Note 1.

Resilience trajectories

The trajectories of recovery for the case study bridge are defined by applying the resilience modeling approach described in the "Methods" section to the six retrofit scenarios for adaptation. For each scenario, functionality-time profiles account for preparatory activities, construction and strengthening phases, and post-intervention administrative procedures required for full-service reinstatement, based on expert-elicited duration estimates and validated against the literature (Further details in Supplementary Note 2). The definition of a reference T_{LC}, for the critical asset at hand, must balance strategic, operational, and societal requirements. Consistent with empirical benchmarks from recent large-scale bridge rehabilitation projects and with operational constraints associated with prolonged closures[57], a control time of 30 months is adopted for the resilience evaluation.

The functionality curves, presented in Fig. 3, highlight distinct recovery trajectories in terms of both duration and timing of restoration steps. The stepwise functionality curves reflect the discrete nature of retrofit implementation, where service functionality changes at identifiable intervention phases, such as closure, partial reopening, traffic management changes, and completion of works. The resilience integral was therefore computed numerically from the discretized functionality time trajectories.

While all strategies satisfy the control time under favorable and median conditions, several scenarios exceed the 30-month threshold under upper-quartile and maximum uncertainty conditions, indicating potential non-compliance with resilience targets. Scenario #3 maintains partial service throughout its intervention period (Fig. 3c), underscoring that resilience is shaped not only by the final restoration time (T_{RE}) but also by the sequencing of recovery steps and the possibility of ensuring a certain level of function throughout the recovery. Furthermore, resilience analysis must consider the expected service life of interventions: strategies leading to prolonged closures and total functionality loss, despite appearing less resilient in the short term, may offer greater long-term sustainability by extending structural lifespan and minimizing future interventions. Supplementary Note 3 reports the variability of these curves, where differences in upper-tail behavior indicate varying robustness to implementation delays and resilience compliance across retrofit strategies. This behavior reflects differing levels of resilience compliance across scenarios. In particular, upper-tail outcomes (Q3 and maximum) indicate that several intervention strategies are likely to exceed acceptable recovery durations under realistic implementation uncertainty.

The proposed framework evaluates resilience primarily in relation to recovery dynamics, intervention implementation, and service continuity under progressive deterioration conditions. The analysis does not explicitly incorporate probabilistic hazard occurrence, fragility relationships, or hazard-dependent structural vulnerability during either the intervention period or the subsequent service life. Consequently, potential differences in future hazard performance among retrofit alternatives (e.g., seismic response) are not explicitly quantified within the present framework. The objective of the study is instead to isolate and compare adaptation and recovery performance associated with alternative intervention strategies. Future developments could integrate hazard-specific fragility and vulnerability modeling to enable combined assessment of long-term adaptation, recovery, and multi-hazard resilience.

Table. 1 | Resilience index (R) and compliance characteristics $P(T_{RE} \le T_{LC})$ (high >75%; moderate 25–75%; low <25%) for the six retrofit scenarios across different assumptions on recovery time

Scenario	Min	Q1	Median (Q2)	Q3	Max	P
#1	0.83	0.73	0.48	$T_{RE} > T_{LC}$	$T_{RE} > T_{LC}$	Moderate
#2	0.80	0.70	0.44	$T_{RE} > T_{LC}$	$T_{RE} > T_{LC}$	Moderate
#3	0.89	0.83	0.66	0.54	$T_{RE} > T_{LC}$	High
#4	0.78	0.58	0.34	$T_{RE} > T_{LC}$	$T_{RE} > T_{LC}$	Low
#5	0.78	0.64	0.34	$T_{RE} > T_{LC}$	$T_{RE} > T_{LC}$	Low
#6	0.81	0.63	0.32	$T_{RE} > T_{LC}$	$T_{RE} > T_{LC}$	Low

Values are shown for minimum, first quartile (Q1), median (Q2), third quartile (Q3), and maximum conditions[a].

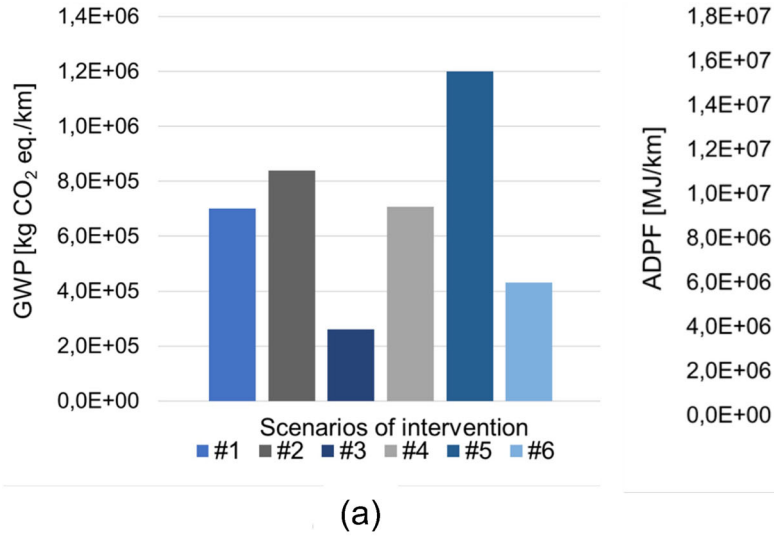
[a]While favorable conditions (Min, Q1) yield high R-indices (typically $R > 0.70$, with Scenario #3 reaching 0.89 at Min and 0.83 at Q1), median values are notably lower (ranging from 0.32 for #6 to 0.66 for #3). Critically, for upper quartiles and maximum conditions, recovery time (T_{RE}) often exceeds the control period (T_{LC}), particularly for all scenarios at Max values and most at Q3 (exceptions: Scenario #3 maintains $R = 0.54$ at Q3 before exceeding T_{LC} at Max). This behavior reflects the uncertainty associated with recovery processes and highlights differences in compliance likelihood across scenarios.

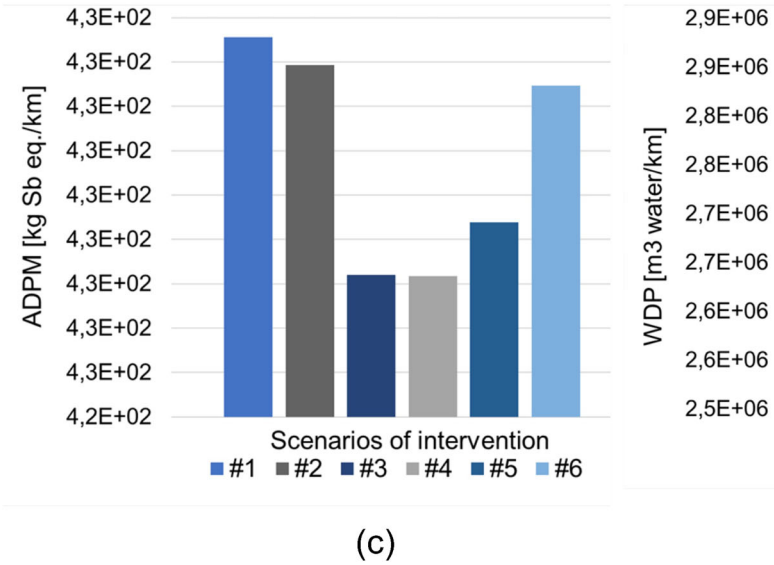
Table 1 summarizes the resilience values obtained for the six retrofit scenarios under different assumptions on recovery time. These results, where scenario #3 consistently suggests a relative advantage in maintaining higher resilience across conditions, corroborate the patterns observed in the functionality curves. Specifically, while all retrofit strategies remain compliant with the control time under average conditions, upper-tail behavior reveals systematic non-compliance with resilience targets for most scenarios. Full deck replacement strategies (scenarios #4–#6) exhibit both lower median resilience and frequent exceedance of the control time under uncertainty, indicating increased risk of unacceptable recovery durations. In contrast, Scenario #3 shows higher resilience and improved compliance across the range of recovery conditions considered, reflecting both faster recovery and reduced sensitivity to implementation delays. These differences highlight that resilience performance depends not only on expected recovery time but also on the likelihood of meeting policy-relevant recovery thresholds.

LCA and LCC evaluations

The following results compare the six retrofit scenarios in terms of life-cycle environmental impacts, costs, and their integration within the multi-criteria decision framework, with full methodological and inventory details provided in Supplementary Note 4. Figure 4 summarizes the life cycle environmental impacts of the six retrofit scenarios across four indicators: global warming potential (GWP), fossil resource use (ADP-fossil), mineral and metal resource use (ADP-mineral), and water depletion potential (WDP), highlighting marked differences among the proposed interventions. These variations underscore the environmental trade-offs inherent in different repair philosophies, with some interventions consistently demonstrating lower overall impacts across multiple categories.

Figure 5 shows the GWP contributions by life-cycle module for each restoration scenario, revealing that the majority of embodied impacts is derived from the upstream manufacturing and material production (modules A1–A3). End-of-life impacts of proposed interventions (C3–C4) are also comparatively higher than those of the original demolished





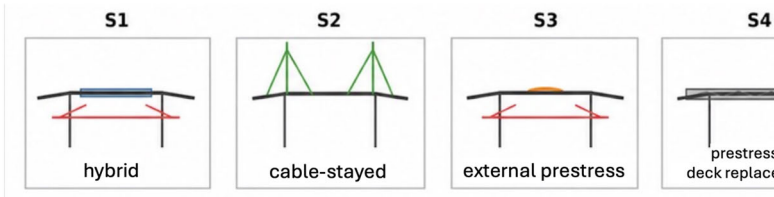


Fig. 4 | Results of environmental impact analysis for six intervention scenarios. **a** GWP; **b** ADPF; **c** ADPM; **d** WDP. Marked differences are observed across scenarios for: **a** global warming potential (GWP), where #5 and #2 show the highest values (≈1.20×10^6 and 8.39×10^5 kg CO_2 eq./km, respectively), while #3 and #6 have the lowest (≈2.61×10^5 and 4.50×10^5 kg CO_2 eq./km). **b** Fossil resource use (ADPF-fossil), with #5 highest (≈1.59×10^7 MJ/km) and #3 and #6 lowest (≈3.33×10^6 and 5.77×10^6 MJ/km). **c** Mineral and metal resource use (ADPM), showing modest differences ($\approx 4.32 \times 10^2$ kg Sb eq./km) with #1 highest and #3 lowest ($\approx 4.27 \times 10^2$ kg Sb eq./km). **d** Water consumption (WDP), ranging from (2.58×10^6 to 2.63×10^6 m^3 water/km) with #5 highest and #4 lowest.

elements, primarily due to greater quantities of new reinforced concrete and structural steel elements introduced.

An analysis of material contributions to the total GWP (Fig. 6) confirms that structural steel, concrete and asphalt binders are the primary drivers of total environmental impacts. This highlights the importance of material selection and design optimization in minimizing the environmental footprint of bridge retrofits.

In Fig. 7, a comparison of direct and indirect costs for the proposed scenarios, indicating a wide range of financial implications, influenced by material choices and the extent of intervention. Direct costs are significantly influenced by manufacturing expenses, as depicted in Fig. 8, with full demolition activities also contributing substantially to module C1 costs. The lowest costs are associated for Scenario #6 and Scenario #3.

Material contribution analysis of direct costs (Fig. 9) further reveals that steel and concrete components primarily drive these expenses, emphasizing the cost sensitivity to material choices in different retrofit designs and highlighting where cost optimization efforts could be most effective.

Two primary cost drivers are identified in the developed LCC model. These are the initial capital costs, i.e., the direct cost of implementing the rehabilitation scenarios corresponding to life cycle modules A1–A3; A5 and the operational costs, due to replacement and maintenance. The latter is governed by module B4, and the service life of elements included in the designed rehabilitation options. In alignment with standard cost estimation and engineering economics protocols (such as the Association for the Advancement of Cost Engineering AACE International Guidelines[58]), the baseline values of these primary cost drivers were varied by 20% (see Supplementary Material, Note 4). It was noted that these variation does not disrupt the final outcomes. Strategy #3 retains its position as the most cost-effective alternative, and Strategy #5 remains the most expensive, across the entire operational uncertainty envelope. Ultimately, it was verified that the baseline economic assumptions and deterministic calculation methods possess a sufficient degree of mathematical robustness.

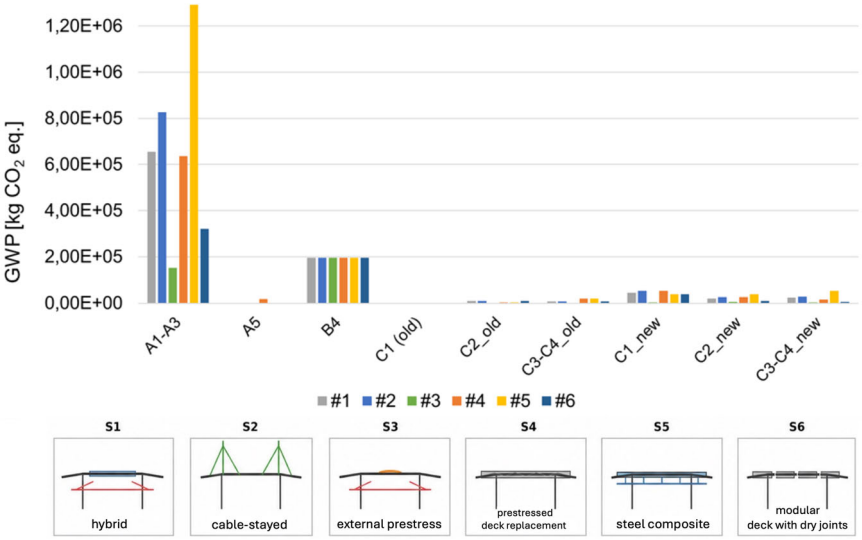


Fig. 5 | GWP contributions by the life cycle module for each intervention scenario. The figure illustrates that the majority of embodied global warming potential (GWP) impacts originate from upstream manufacturing and material production (modules *A1–A3*) and Replacement (B4). End-of-life impacts (*C3–C4*) of the proposed interventions generally exceed those of the original demolished bridge elements, a consequence of increased use of reinforced concrete and structural steel in new solutions. Replacement (B4) contributes approximately 2×10^5 kg CO_2 eq. across all intervention scenarios.

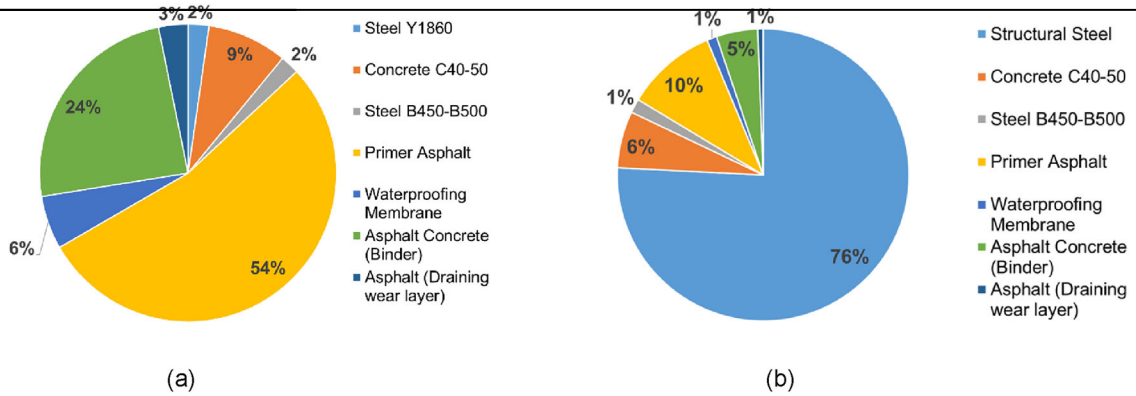


Fig. 6 | Material composition breakdown for contribution to GWP for structural interventions. Examples for scenarios #3 (**a**) and #5 (**b**). The figure highlights that structural steel, asphalt binder and concrete are the primary drivers of total GWP. For Scenario #5 (**b**), structural steel components contribute 76% of the total GWP for the new superstructure. In Scenario #3 (**a**), approximately 54% of the GWP is attributable to the selected primer asphalt works.

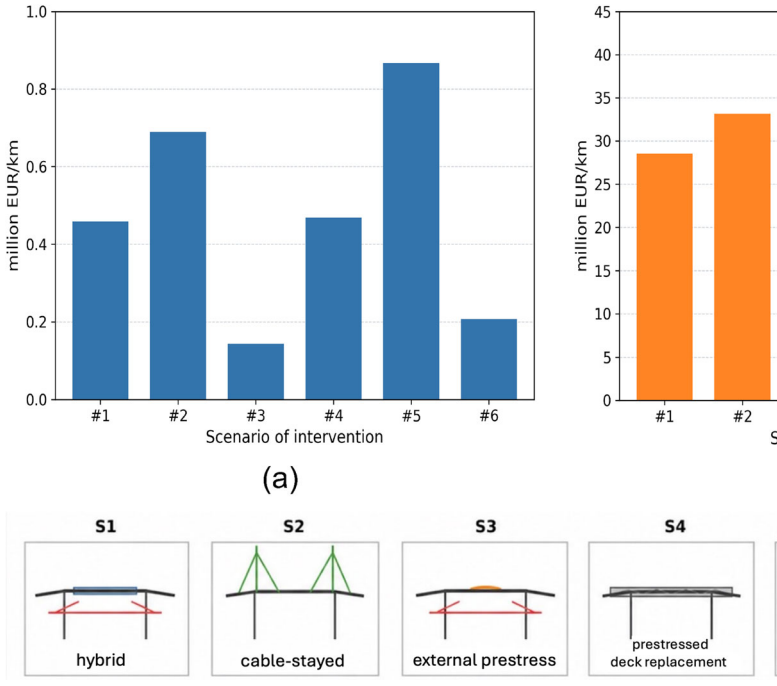


Fig. 7 | Comparison of **a** direct costs and **b** indirect costs across designed intervention scenarios. Direct costs (**a**) represent the cost of materials, labor and machinery. Scenario #5 (steel superstructure) incurs the highest direct costs (1960,000 EUR/km), followed by #2 (1950,000 EUR/km). Scenarios #1 and #4 are similar (634,000 EUR/km and 648,000 EUR/km), while #6 (prefabricated segments) and #3 show the lowest costs (200,000 EUR/km and 289,000 EUR/km, respectively). In direct costs (**b**), associated with disruptions and vehicle detours, also showcase

Decision optimization

The multi-criteria decision analysis integrates four performance dimensions—resilience, life-cycle cost, life-cycle environmental impact, and expected service life. All criteria are derived from the case-study analyses presented in Supplementary Note 1 and are combined following the decision framework introduced in the "Methods" section. In the case-study application, resilience components are combined using weights of 0.7 for the median recovery trajectory ($Q2$) and 0.3 for the upper quartile ($Q3$). Life-cycle costs are expressed as an aggregated index per kilometer of bridge, with direct intervention costs and indirect user costs assigned equal weights of 0.5 each in the baseline configuration; alternative weightings are subsequently explored to assess sensitivity to stakeholder priorities. Environmental impact categories are aggregated using Joint Research Centre–recommended weights (0.46 for GWP, 0.17 for ADPM, 0.18 for ADPF, and 0.19 for WDP) enabling transparent aggregation and subsequent sensitivity analysis. Expected service life L_i is included as a separate dimension to account for differences in long-term durability among retrofit strategies.

The resulting normalized multi-criteria representation defines the decision space used for comparative appraisal of the six scenarios (Fig. 10), where cost and environmental impact are minimized, and resilience and expected service life are maximized under the adopted weighting assumptions. The decision problem minimizes economic and environmental impacts while maximizes resilience and service life. Accordingly, the multi-objective optimization is formulated as defined in Eq. 11 to identify strategies that achieve favorable trade-offs across these competing dimensions, subject to technical, operational, and policy constraints, such as budget limits, minimum resilience requirements, serviceability criteria, and regulatory thresholds. In this formulation, the control time acts as a policy-relevant threshold rather than a strict feasibility constraint. Scenarios exceeding T_{LC} are retained within the decision space but are penalized through their resilience scores and compliance characteristics, enabling explicit evaluation of trade-offs between short-term recovery performance and long-term system benefits.

Ranking of the retrofitting strategies and the sensitivity analysis

The final ranking is presented in Table 2, which reports the UPI and TOPSIS method results for the baseline case and for four alternative weighting schemes prioritizing economic, environmental, resilience, and service-life dimensions. The baseline scenario corresponds to $T1$, while the four test scenarios, $T2$–$T5$, prioritize economic ($T2$), environmental ($T3$), resilience ($T4$), and service-life ($T5$) objectives (see "Methods" for full weight vectors). By adjusting these weights, the UPI formulation (Eq. 12) can capture different policy priorities. For example, assigning a higher value to w_R emphasizes resilience, w_L brings the priority to service life extension, while larger w_E or w_C highlight environmental or economic concerns. The robustness of these results is further examined using the TOPSIS method (Eq. 15). Table 2 reports CC_i-based proximity to the ideal and thus a superior rank of the six intervention scenarios (#1–#6) under five weighting schemes ($T1$–$T5$).

Both the UPI and TOPSIS are compatible and complementary: each permits explicit specification of preference weights, enabling consistent comparison of alternative solutions. The UPI delivers a transparent, easily communicable scalarization that is advantageous when interpretability and stakeholder engagement are paramount. TOPSIS, by contrast, offers a geometric assessment based on proximity to an ideal and distance from an anti-ideal solution, which can better reveal trade-offs and rank ordering when the decision space is skewed or non-compensatory effects are important. Applying both methods in parallel, and subjecting their outcomes to systematic sensitivity analysis, therefore, provides cross-validation of rankings, highlights cases of methodological divergence, and strengthens confidence in the final selection.

The comparative analysis (Table 2) reveals robust, policy-dependent ranking patterns that illuminate the trade-offs inherent in retrofit decision-making. Across aggregation methods, interventions #3, #4 and #6 emerge as the most competitive, but their relative dominance shifts with the prioritized

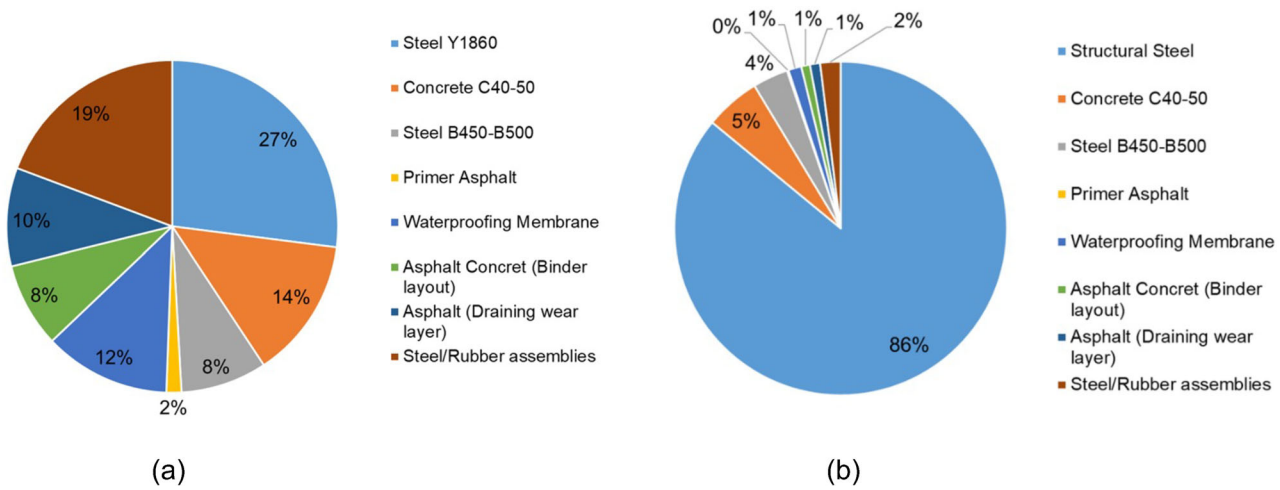


Fig. 9 | Material contribution breakdown of direct costs for structural interventions (manufacturing stage only). Examples for scenarios #3 (**a**) and #5 (**b**). The figure illustrates that steel, steel assemblies and concrete components are the primary drivers of direct costs. For Scenario #5 (**b**), which yields the highest overall costs, approximately 86% of expenses stem from structural steel elements of the superstructure. In Scenario #3 (**a**), which involves high-strength steel cables and a new concrete deck, high-strength steel cables account for 27% of direct costs, concrete works contribute about 14%, and steel reinforcement bars 8%.

objective, reflecting structural differences in recovery performance, longevity and environmental footprint. In detail, under equal weighting ($T1$), both UPI and TOPSIS identify Scenario #6 as the leading candidate, followed closely by scenarios #3 and #4. This baseline result indicates that, when no single objective is privileged, strategies combining extended service life with acceptable resilience and life cycle impacts tend to be preferred. The concordance between UPI and TOPSIS in the top three under $T1$ supports the robustness of this observation. When economic objectives ($T2$) are prioritized, Scenario #6 remains the top performer, with Scenario #4 following. Under environmental performance ($T3$) and resilience ($T4$) prioritization, Scenario #3 emerges as the leading option, while Scenario #6 ranks second. In contrast, under service-life prioritization ($T5$), scenarios #6 and #4 lead decisively. These outcomes reflect the fundamentally different strengths of the retrofit strategies. Replacement-oriented solutions, such as scenarios #6 and #4, benefit from the extended service life, which strongly improves their performance. By contrast, strengthening- and hybrid-based interventions, exemplified by Scenario #3, are favored when resilience and environmental performance are prioritized, owing to shorter recovery times, reduced construction impacts, and lower exposure to prolonged service disruption. The ranking patterns, therefore, illustrate how the preferred intervention shifts depending on whether decision-makers emphasize, e.g., short-term recovery and robustness, or long-term asset renewal and longevity.

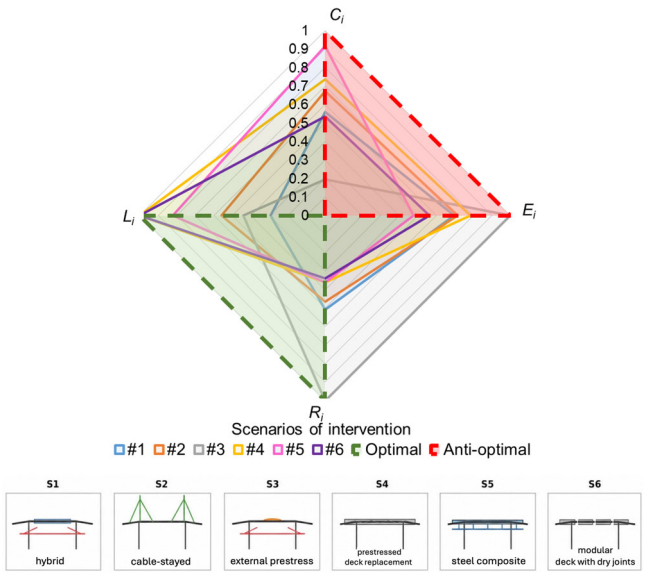


Fig. 10 | Multi-criteria decision space for retrofit strategy selection. Normalized multi-criteria representation of the retrofit scenarios, minimizing cost (C_i) and environmental impact (E_i) while maximizing resilience (R_i) and service life (L_i). Each marker corresponds to a retrofit scenario (#1–#6), positioned according to its normalized performance across the considered criteria. The shaded region identifies the subset of solutions that achieve favorable trade-offs across all objectives under the selected weighting scheme, defining the preferred decision space. Axes represent normalized criteria values, with higher values indicating improved performance. The green dashed region indicates the preferred decision space, whereas the red dashed region represents non-optimal solutions.

A supplementary sensitivity analysis was additionally performed to evaluate the influence of the selected control time (T_{LC}) on the ranking outcomes by considering alternative recovery horizons of 24 and 36 months. The results confirm that the framework responds systematically and transparently to different recovery-policy assumptions. Shorter control times penalize interventions associated with prolonged recovery trajectories, whereas longer recovery horizons increase the relative attractiveness of strategies offering extended service life and long-term renewal benefits. Importantly, despite variations in absolute rankings, the overall strategic trade-off structure remains broadly consistent across T_{LC} assumptions. The sensitivity analysis shows that the effect of T_{LC} is reflected primarily through the resilience criterion, while the final MCDA rankings remain governed by trade-offs among all evaluation criteria. Scenario #3 consistently exhibits the strongest recovery-resilience performance; however, it does not always achieve the highest overall MCDA score because, even under the resilience-oriented weighting scheme substantially weight is still assigned to life-cycle cost, environmental impact and expected service life. This distinction explains why replacement-oriented solutions, particularly Scenario #4, may remain competitive or become preferred under certain T_{LC} assumptions, as their superior long-term service-life performance can offset weaker recovery performance. Full results of the sensitivity analysis are provided in Supplementary Note 5.

Conclusions

We developed a decision-oriented methodology that reframes infrastructure adaptation as a policy-sensitive optimization problem rather than a purely technical exercise. By explicitly integrating variable recovery-resilience trajectories with life cycle environmental and economic assessments within a transparent multi-criteria decision structure, we moved beyond static performance comparisons. The core innovation of this approach lies in operationalizing resilience as a recovery-based, time-bounded, and uncertainty-aware decision variable linked to retrofit implementation that can be directly weighed against carbon, cost, and longevity. This enables trade-offs to be interrogated rather than obscured. In doing so, the methodology bridges a critical gap between engineering analysis and strategic infrastructure governance.

Table. 2 | Results of the multi-criteria analysis of intervention solutions (for T_{LC} = 30 months)

Method:	**UPI**					**TOPSIS**				
Scenario	J_i ($T1$)	J_i ($T2$)	J_i ($T3$)	J_i ($T4$)	J_i ($T5$)	CC_i ($T1$)	CC_i ($T2$)	CC_i ($T3$)	CC_i ($T4$)	CC_i ($T5$)
#1	0.378	0.389	0.349	0.431	0.345	0.382	0.391	0.352	0.433	0.356
#2	0.379	0.311	0.341	0.414	0.451	0.389	0.326	0.350	0.419	0.481
#3	**0.558**	**0.628**	0.329	**0.729**	0.506	**0.531**	**0.592**	0.398	**0.642**	0.579
#4	0.455	0.370	0.359	0.417	0.673	0.468	0.400	0.393	0.434	0.665
#5	0.447	0.302	0.477	0.412	0.597	0.459	0.352	0.481	0.426	0.580
#6	**0.551**	0.501	**0.505**	0.466	**0.730**	**0.540**	0.501	**0.504**	0.472	**0.695**

Weighting schemes: $T1$-baseline, $T2$-economic, $T3$-environmental, $T4$-resilience, $T5$: service-life.

The application to a real, ageing bridge suggests that retrofit decisions for adaptation are shaped by competing objectives and are contingent on societal objectives and context specific constraints. The results show that no single retrofit solution is universally preferred across all policy perspectives. For example, interventions that preserve and strengthen existing structures emerge as superior when rapid recovery, emissions reduction, and service continuity are prioritized. By contrast, replacement strategies gain relevance only when long-term durability is dominant despite higher near-term disruption. Thus, resilience-recovery compliance cannot be inferred from average outcomes alone: upper-tail recovery behavior determines whether policy targets are met under realistic implementation uncertainty. Strategies that combine short and predictable recovery trajectories with limited dispersion, therefore, offer a more robust basis for public investment in critical infrastructure. Sensitivity analyses further highlight that the proposed framework responds coherently to alternative recovery-policy assumptions, enabling context-dependent prioritization of retrofit strategies under varying operational requirements.

The proposed formulation provides a scalable decision support tool for infrastructure owners and regulators facing accelerating climate, budgetary, and operational pressures. By making value judgements explicit—through weights, control times, and uncertainty thresholds—the framework enables transparent and interpretable alignment between engineering choices and policy objectives, from decarbonization to network reliability. This positions resilience not as an abstract aspiration, but as a measurable and governable property of infrastructure systems.

The proposed framework is transferable and thus can be implemented to diverse critical infrastructure, yet, the resulting rankings are case-specific. Hence, its application to other infrastructure typologies or regional contexts would require appropriate case-specific calibration and input data, including structural configuration, deterioration and hazard models, adaptation strategies, environmental inventories, economic parameters, and regulatory constraints. Future work would also explore alternative integration strategies, including outranking methods, robust decision making, and participatory multi-attribute utility approaches, to further address the theoretical challenges associated with aggregating incommensurable resilience, environmental, economic, and durability criteria. Integration with digital twins, remote sensing, and near-real-time monitoring could further embed this approach into adaptive asset management, supporting evidence-based prioritization across ageing bridge networks at regional and national scales. Further developments could also explore the integration of larger empirical recovery datasets, probabilistic hazard modeling, and monitoring data to further enhance the predictive and generalizable capabilities of the framework.

Data availability

The datasets generated and analyzed during the current study, including the resilience assessment results, life-cycle assessment (LCA) and life-cycle cost (LCC) inventories and outputs, and multi-criteria decision analysis (MCDA) results, are currently stored by the corresponding author and are available from the corresponding author (Stergios-Aristoteles Mitoulis; s.mitoulis@ucl.ac.uk) upon reasonable request.

Received: 1 February 2026; Accepted: 15 September 2026;
Published online: 07 October 2026

References

1. Galasso, C., McNair, J., Fujii, M. & Dong, Z. Resilient infrastructure. *Commun. Eng.* **1**, 27 https://doi.org/10.1038/s44172-022-00032-5 (2022).
2. Esmalian, A. et al. Operationalizing resilience practices in transportation infrastructure planning and project development. *Transp. Res. Part D* **104**, 103214 https://doi.org/10.1016/j.trd.2022.103214 (2022).
3. Forcellini, D. & Mitoulis, S. A. Effect of deterioration on critical infrastructure resilience – framework and application on bridges. *Results Eng.* **25**, 103834 https://doi.org/10.1016/j.rineng.2024.103834 (2025).
4. Ouyang, M., Cheng, Z., Ma, J., Wang, H. & Mitoulis, S. A. Coupled urban risks: a complex systems perspective with a people-centric focus. *Engineering* **44**, 44–50 https://doi.org/10.1016/j.eng.2024.12.023 (2024).
5. Kopiika, N., Di Bari, R., Argyroudis, S., Ninic, J. & Mitoulis, S. A. Sustainability and resilience-driven prioritisation for restoring critical infrastructure after major disasters and conflict. *Transp. Res. Part D* 104592 https://doi.org/10.1016/j.trd.2025.104592 (2025).
6. Kopiika, N., Robery, P., Ninić, J. & Mitoulis, S. A. Quantifying structural deterioration for sustainable development: the importance of climate adaptation of existing critical infrastructure. *Case Stud. Constr. Mater.* **22**, e04757 https://doi.org/10.1016/j.cscm.2025.e04757 (2025).
7. Dulin, S. et al. Rethinking infrastructure design from component failure to systemic resilience. *Nat. Commun.* **16**, 9681 https://doi.org/10.1038/s41467-025-64683-6 (2025).
8. Al Jazeera and News Agencies. Francis Scott Key Bridge collapse updates http://surl.li/quivrh (last accessed 22 October 2025).
9. Calvi, G. M. et al. Once upon a time in Italy: the tale of the Morandi Bridge. *Struct. Eng. Int.* **29**, 198–217 https://doi.org/10.1080/10168664.2018.1558033 (2018).
10. Domaneschi, M. et al. Collapse analysis of the Polcevera Viaduct by the applied element method. *Eng. Struct.* **214**, 110659 https://doi.org/10.1016/j.engstruct.2020.110659 (2020).
11. Roostaie, S., Nawari, N. & Kibert, C. J. Integrated sustainability and resilience assessment framework: from theory to practice. *J. Clean. Prod.* **232**, 144–156 https://doi.org/10.1016/j.jclepro.2019.05.382 (2019).
12. Mitoulis, S.-A., Kopiika, N., Di Bari, R. & Argyroudis, S. Sustained resilience as a unifying property of cities and the built environment. *NPJ Urban Sustain.* https://doi.org/10.1038/s42949-026-00457-3 (2026).
13. Wang, D. et al. Analysis of land system resilience: static and dynamic perspectives. *J. Clean. Prod.* **447**, 141702 https://doi.org/10.1016/j.jclepro.2024.141258 (2024).
14. Tafur, A., Argyroudis, S. A., Mitoulis, S. A. & Pargett, J. Climate-resilient railway networks: a resource-aware framework. *Commun. Eng.* **4**, 157 https://doi.org/10.1038/s44172-025-00493-4 (2025).
15. Wiedenhofer, D. et al. Mapping and modelling global mobility infrastructure stocks, material flows and their embodied greenhouse gas emissions. *J. Clean. Prod.* **434**, 140161 https://doi.org/10.1016/j.jclepro.2023.139742 (2024).
16. Di Bari, R., Cucuzza, R., Domaneschi, M. & Mitoulis, S. A. Enhancing sustainability and resilience against natural hazard of the built environment—state of the art and development of a novel framework. *Sustain. Dev.* **33** https://doi.org/10.1002/sd.70150 (2025).
17. Tapia, C. & Padgett, J. E. Multi-objective optimisation of bridge retrofit and post-event repair selection to enhance sustainability. *Struct. Infrastruct. Eng.* **12**, 93–107 https://doi.org/10.1080/15732479.2014.995676 (2016).
18. Bocchini, P. & Frangopol, D. M. Restoration of bridge networks after an earthquake: multicriteria intervention optimization. *Earthq. Spectra* **28**, 427–455 https://doi.org/10.1193/1.4000019 (2012).
19. Dong, Y. & Frangopol, D. M. Performance-based seismic assessment of conventional and base-isolated steel buildings including environmental impact and resilience. *Earthq. Eng. Struct. Dyn.* **45**, 739–756 https://doi.org/10.1002/eqe.2682 (2016).
20. Kazantzi, A. K., Moutsianos, S., Bakalis, K. & Mitoulis, S. A. Cause-agnostic bridge damage state identification utilising machine learning. *Eng. Struct.* **320**, 118887 https://doi.org/10.1016/j.engstruct.2024.118887 (2024).
21. Markogiannaki, O., Xu, H., Chen, F., Mitoulis, S. A. & Parcharidis, I. Monitoring of a landmark bridge using SAR interferometry coupled

with engineering data and forensics. *Int. J. Remote Sens.* **43**, 95–119 https://doi.org/10.1080/01431161.2021.2003468 (2022).
22. Li, F., Luo, D. & Niu, D. Data-intelligence driven methods for durability, damage diagnosis and performance prediction of concrete structures. *Commun. Eng.* **4**, 100 https://doi.org/10.1038/s44172-025-00431-4 (2025).
23. Tzortzinis, G. et al. Structural integrity of aging steel bridges by 3D laser scanning and convolutional neural networks. *Commun. Eng.* **3**, 106 https://doi.org/10.1038/s44172-024-00255-8 (2024).
24. Kopiika, N. et al. Rapid post-disaster infrastructure damage characterisation using remote sensing and deep learning technologies: a tiered approach. *Autom. Constr.* **170**, 105955 https://doi.org/10.1016/j.autcon.2024.105955 (2025).
25. Domaneschi, M. et al. Resilience analysis of different retrofitting solutions for a prestressed concrete viaduct. *Procedia Struct. Integr.* **62**, 1028–1035 https://doi.org/10.1016/j.prostr.2024.09.137 (2024).
26. Domaneschi, M. et al. Resilience and sustainability assessment of a prestressed concrete viaduct. In *Bridge Maintenance, Safety, Management, Digitalization and Sustainability – Proc. IABMAS 2024*, 2594–2602 (CRC Press, 2024).
27. Xu, L. Y. et al. Green and low-carbon matrices for engineered/strain-hardening cementitious composites (ECC/SHCC): towards sustainable and resilient infrastructure. *J. Clean. Prod.* 144968 https://doi.org/10.1016/j.jclepro.2025.144968 (2025).
28. Zheng, X., Liu, Q., Li, Y., Wang, B. & Qin, W. Safety risk assessment for connected and automated vehicles: integrating FTA and CM-improved AHP. *Reliab. Eng. Syst. Saf.* **257**, 110822 https://doi.org/10.1016/j.ress.2025.110822 (2025).
29. Chang, Y. T. & Hsieh, S. H. Development and application of an enhanced building circularity indicator: a pilot study in Taiwan. *J. Clean. Prod.* 145363 https://doi.org/10.1016/j.jclepro.2025.145363 (2025).
30. Cózar, J. C. G., García-Martínez, A., Merino, B. M., Tovar, J. A. C. & Rey-Álvarez, B. An approach to using life cycle assessment generative algorithm in buildings: optimisation of BIM models during the early design phase. *J. Clean. Prod.* **530**, 146847 https://doi.org/10.1016/j.jclepro.2025.146847 (2025).
31. Cheng, M., Huang, Z. & Zheng, Y. A review on life-cycle carbon emissions of reinforced concrete buildings: calculation and reduction. *J. Clean. Prod.* **526**, 146501 https://doi.org/10.1016/j.jclepro.2025.146501 (2025).
32. Ayyub, B. M. Disaster resilience and sustainability of infrastructures: relationships and quantification methods. in *Gulf Conference on Sustainable Built Environment*, 289–308 https://doi.org/10.1007/978-3-030-39734-0_18 (Springer International Publishing, 2020).
33. Ayyub, B. M. Infrastructure resilience and sustainability: definitions and relationships. *ASCE ASME J. Risk Uncertain. Eng. Syst. Part A Civ. Eng.* **6**, 02520001 https://doi.org/10.1061/AJRUA6.0001067 (2020b).
34. Sánchez-Silva, M. et al. Moving toward resilience and sustainability in the built environment. *Struct. Saf.* **113**, 102449 https://doi.org/10.1016/j.strusafe.2024.102449 (2025).
35. OECD. Recommendation of the Council on the Governance of Infrastructure, OECD/LEGAL/0460 (OECD, 2025).
36. Hallegatte, S., Rentschler, J. & Rozenberg, J. *Lifelines: The Resilient Infrastructure Opportunity* https://openknowledge.worldbank.org/entities/publication/c3a753a6-2310-501b-a37e-5dcab3e96a0b (World Bank Publications, 2019).
37. EU Adaptation Strategy https://climate-adapt.eea.europa.eu/en/eu-adaptation-policy/strategy (2021).
38. Faber, M. H., Miraglia, S., Qin, J. & Stewart, M. G. Bridging resilience and sustainability – decision analysis for design and management of infrastructure systems. *Sustain. Resilient Infrastruct.* **5**, 102–124 https://doi.org/10.1080/23789689.2017.1417348 (2020).
39. ReCharged – Climate-aware Resilience for Sustainable Critical and Interdependent Infrastructure Systems enhanced by Emerging Digital Technologies. Horizon Europe Project No. 101086413 (2021).
40. Frangopol, D. M., Dong, Y. & Sabatino, S. Bridge life-cycle performance and cost: analysis, prediction, optimisation and decision-making. in *Structures and Infrastructure Systems,* 66–84 (Routledge, 2019).
41. O'Hagan, A. et al. *Uncertain Judgements: Eliciting Experts' Probabilities* https://doi.org/10.1002/0470033312 (2006).
42. Aspinall, W. P. & Cooke, R. M. Quantifying scientific uncertainty from expert judgement elicitation. in (Rougier, J., Sparks, S. & Hill, L. J. eds) *Risk and Uncertainty Assessment for Natural Hazards*, 64–99 https://doi.org/10.1017/CBO9781139047562.005 (Cambridge University Press, 2013).
43. Hemming, V., Burgman, M., Hanea, A., McBride, M. & Wintle, B. A practical guide to structured expert elicitation using the IDEA protocol. *Methods Ecol. Evol.* **9**, 169–180 https://doi.org/10.1111/2041-210X.12857 (2017).
44. Mitoulis, S. A., Argyroudis, S. A., Loli, M. & Imam, B. Restoration models for quantifying flood resilience of bridges. *Eng. Struct.* **238**, 112180 (2021).
45. Bruneau, M. et al. A framework to quantitatively assess and enhance the seismic resilience of communities. *Earthq. Spectra* **19**, 733–752 https://doi.org/10.1193/1.1623497 (2003).
46. Cimellaro, G. P., Reinhorn, A. M. & Bruneau, M. Framework for analytical quantification of disaster resilience. *Eng. Struct.* **32**, 3639–3649 https://doi.org/10.1016/j.engstruct.2010.08.008 (2010).
47. AASHTO. Guide Specifications for Bridges Vulnerable to Coastal Storms. (American Association of State Highway and Transportation Officials, 2020).
48. FHWA. Transportation System Resilience to Extreme Weather and Climate Change, FHWA-HEP-17-082 (Federal Highway Administration, 2017).
49. MIT/ANSFISA. Linee Guida per la Classificazione e Gestione del Rischio, la Valutazione della Sicurezza ed il Monitoraggio dei Ponti Esistenti, DM 578/2020. (Ministero delle Infrastrutture e dei Trasporti, Agenzia Nazionale per la Sicurezza delle Ferrovie e delle Infrastrutture Stradali e Autostradali, 2020).
50. Loli, M., Kefalas, G., Dafis, S., Mitoulis, S. A. & Schmidt, F. Bridge-specific flood risk assessment of transport networks using GIS and remotely sensed data. *Sci. Total Environ.* **850**, 157976 (2022).
51. PIARC. *Resilience of Road Transport Systems to Major Disasters*. World Road Association (PIARC), Technical Committee B.4 (PIARC, 2019).
52. EN 15804. Sustainability of construction works—Environmental product declarations—Core rules for the product category of construction products (2012).
53. EN 15978. Sustainability of construction works—Assessment of environmental performance of buildings—Calculation method (2011).
54. Sala, S., Cerutti, A. & Pant, R. *Development of a Weighting Approach for the Environmental Footprint*, EUR 28562 EN https://doi.org/10.2760/945290 (Publications Office of the European Union, 2017).
55. Behzadian, M., Otaghsara, S. K., Yazdani, M. & Ignatius, J. A state-of the-art survey of TOPSIS applications. *Expert Syst. Appl.* **39**, 13051–13069 https://doi.org/10.1016/j.eswa.2012.05.056 (2012).
56. Zyoud, S. H. & Fuchs-Hanusch, D. A bibliometric-based survey on AHP and TOPSIS techniques. *Expert Syst. Appl.* **78**, 158–181, https://doi.org/10.1016/j.eswa.2017.02.016 (2017).
57. Beaver, E. & Mitoulis, S. A. Evidence-based flood resilience models for bridges. *Proc. Inst. Civ. Eng. Bridge Eng.* 1–15 https://doi.org/10.1680/jbren.24.00039 (2024).
58. Professional Guidance Documents, AACE International is the Association for the Advancement of Cost Engineering https://web.aacei.org/resources/professional-guidance-documents

59. ISO 14040. Environmental management—Life cycle assessment—Principles and framework (2006).
60. ISO 15686-5. Buildings and constructed assets—Service life planning—Life-cycle costing (2017).
61. ISO 14044 Environmental management—Life cycle assessment—Requirements and guidelines (2006).

Acknowledgements

The authors gratefully acknowledge the following experts, who participated in the questionnaire and provided valuable contributions to this study, and who have given their explicit consent to be mentioned here. Prof. José Turmo (UPC BARCELONATECH), Prof. Xiaowei Wang (Tongji University), Prof. Jun Yang (Chongqing Jiaotong University), Dr. Francesco Presta (Technical Director at BG&E), Dr. Francesco Fanigliulo (Principal FaniPro), Prof. Henrry Rojas (Pontifical Catholic University of Chile), Dr. Konstantinos Katirtzoglou (Principal Engineer, Four-Tees Engineers Ltd), Dr. Andrea Caristo (Associate Director – AECOM). The contribution of Paolo Baiardi (Chief Operating Officer – SALT AUTOCISA, ASTM GROUP COMPANY), who provided valuable support in assessing the construction operations and intervention procedures, is gratefully acknowledged. The authors also gratefully acknowledge the contribution of Dr. Raffaele Cucuzza (Politecnico di Torino) in the preparation of the questionnaire. Nadiia Kopiika would like to acknowledge of support received from the British Academy for this research (Award Reference: RaR\100770).

Author contributions

Marco Domaneschi: conceptualization, data curation, formal analysis, investigation, methodology, project administration, software, supervision, validation, visualization, writing-original draft, writing-review & editing. Nadiia Kopiika: data curation, formal analysis, investigation, software, validation, visualization, writing-original draft, writing-review & editing. Roberta Di Bari: data curation, formal analysis, investigation, methodology, software, validation, visualization, writing-original draft, writing-review & editing. Paola Cavallaro: data curation, formal analysis, investigation, software, visualization, writing-original draft, writing-review & editing. Valentina Villa: data curation, formal analysis, investigation, methodology, validation, visualization, writing-original draft, writing-review & editing. Sotirios Argyroudis: conceptualization, data curation, formal analysis, investigation, methodology, project administration, supervision, funding acquisition, visualization, writing-original draft, writing-review & editing. Stergios-Aristoteles Mitoulis: conceptualization, funding acquisition, investigation, methodology, project administration, supervision, validation, visualization, writing-review & editing.

Funding

This research was funded by the European Union HORIZON-MSCA-2021-SE-01 (101086413) “ReCharged – Climate-aware resilience for sustainable critical and interdependent Infrastructure systems enhanced by emerging digital technologies” and the UK Research and Innovation (UKRI) under the UK government’s Horizon Europe funding guarantee (EP/Y003586/1, EP/X037665/1).

Competing interests

The authors declare no competing interests.

Additional information

Supplementary information The online version contains supplementary material available at https://doi.org/10.1038/s44172-026-00794-2.

Correspondence and requests for materials should be addressed to Stergios-Aristoteles Mitoulis.

Peer review information *Communications Engineering* thanks all reviewer(s) for their contribution to the peer review of this work. Primary handling editors: [Danielle Densley Tingley] and [Philip Coatsworth]. A peer review file is available.

Reprints and permissions information is available at http://www.nature.com/reprints

Publisher’s note Springer Nature remains neutral with regard to jurisdictional claims in published maps and institutional affiliations.

Open Access This article is licensed under a Creative Commons Attribution 4.0 International License, which permits use, sharing, adaptation, distribution and reproduction in any medium or format, as long as you give appropriate credit to the original author(s) and the source, provide a link to the Creative Commons licence, and indicate if changes were made. The images or other third party material in this article are included in the article's Creative Commons licence, unless indicated otherwise in a credit line to the material. If material is not included in the article's Creative Commons licence and your intended use is not permitted by statutory regulation or exceeds the permitted use, you will need to obtain permission directly from the copyright holder. To view a copy of this licence, visit http://creativecommons.org/licenses/by/4.0/.

© Crown 2026

This Article in Press is shared early to give you faster access to new research. It is citable and carries a permanent DOI. The final edited version will replace it automatically.